Received: 31 October 2023 | Revised: 15 February 2024 | Accepted: 29 February 2024

DOI: 10.1002/lio2.1247

ORIGINAL RESEARCH

Laryngoscope Investigative Otolaryngology

Dynamic flow for efficient partial decellularization of tracheal grafts: A preliminary rabbit study

Woo Yul Byun BSE[1,2] | Lumei Liu PhD[2] | Amanda Palutsis MS[2,3] | Zheng Hong Tan PhD[1,2] | Rachel Herster MSE[3,4] | Kyle VanKoevering MD[4] | Amy Manning MD[2,5] | Tendy Chiang MD[2,5]

[1]College of Medicine, The Ohio State University, Columbus, Ohio, USA

[2]Center for Regenerative Medicine, Abigail Wexner Research Institute, Nationwide Children's Hospital, Columbus, Ohio, USA

[3]College of Engineering, The Ohio State University, Columbus, Ohio, USA

[4]Department of Otolaryngology–Head & Neck Surgery, The Ohio State University Medical Center, Columbus, Ohio, USA

[5]Department of Pediatric Otolaryngology, Nationwide Children's Hospital, Columbus, Ohio, USA

Correspondence
Tendy Chiang, Center for Regenerative Medicine, Abigail Wexner Research Institute, Nationwide Children's Hospital, 555 S. 18th Street, Suite 2A, Columbus, OH 43205-2664, USA.
Email: tendy.chiang@nationwidechildrens.org

Funding information
Alpha Omega Alpha Carolyn L. Kuckein Student Research Fellowship; National Heart, Lung, and Blood Institute, Grant/Award Number: R01HL157039

Abstract

Objective: Bioengineered tracheal grafts are a potential solution for the repair of long-segment tracheal defects. A recent advancement is partially decellularized tracheal grafts (PDTGs) which enable regeneration of host epithelium and retain viable donor chondrocytes for hypothesized benefits to mechanical properties. We propose a novel and tunable 3D-printed bioreactor for creating large animal PDTG that brings this technology closer to the bedside.

Methods: Conventional agitated immersion with surfactant and enzymatic activity was used to partially decellularize New Zealand white rabbit (*Oryctolagus cuniculus*) tracheal segments ($n = 3$). In parallel, tracheal segments ($n = 3$) were decellularized in the bioreactor with continuous extraluminal flow of medium and alternating intraluminal flow of surfactant and medium. Unprocessed tracheal segments ($n = 3$) were also collected as a control. The grafts were assessed using the H&E stain, tissue DNA content, live/dead assay, Masson's trichrome stain, and mechanical testing.

Results: Conventional processing required 10 h to achieve decellularization of the epithelium and submucosa with poor chondrocyte viability and mechanical strength. Using the bioreactor reduced processing time by 6 h and resulted in chondrocyte viability and mechanical strength similar to that of native trachea.

Conclusion: Large animal PDTG created using our novel 3D printed bioreactor is a promising approach to efficiently produce tracheal grafts. The bioreactor offers flexibility and adjustability favorable to creating PDTG for clinical research and use.

Presented at the Combined Otolaryngology Spring Meeting, Boston, Massachusetts, USA, May 3–7, 2023.

Future research includes optimizing flow conditions and transplantation to assess post-implant regeneration and mechanical properties.

Level of Evidence: NA.

KEYWORDS
bioreactor, chondrocyte viability, regenerative medicine, tissue engineering, tracheal replacement

1 | INTRODUCTION

An ideal solution to repairing long-segment tracheal defects does not yet exist. Long-segment tracheal disease can be life-threatening because they compromise the airway and cause recurrent airway infections.[1,2] In rare cases, tracheal replacement is needed. The requirements for an ideal tracheal replacement include low immunogenicity to prevent rejection, structural integrity to maintain airway patency, and a functional respiratory epithelium.

Although there have been some successes with current options for tracheal replacement, they have shortcomings in one or more of these requirements. Autologous tracheal reconstruction is often a heroic measure with variable clinical outcomes and constructs that lack the properties of the original trachea.[3–6] Allogeneic tracheal replacement requires immunosuppression, management of a complex blood supply, and is limited in availability.[7,8] Similarly, synthetic tracheal replacements have a significant risk of foreign body reaction and often fail to epithelialize, revascularize, and remain patent.[9,10] Using decellularized allogeneic trachea can address some of these shortcomings. Reconstruction with a decellularized allogenic trachea removes immunogenic cellular material while maintaining a native extracellular matrix (ECM) that can aid in graft regeneration. However, complete decellularization often results in the loss of a patent airway since viable chondrocytes contribute to the long-term structural integrity of the trachea.[11]

A novel approach that may address these shortcomings is partial decellularization. The goal of partial decellularization is to completely decellularize the epithelium and submucosa while preserving cartilage and its immunoprivileged chondrocytes. The antigenicity of partial decellularized tracheal grafts can be greatly reduced by removing the epithelium and mixed glands.[12] Many studies have shown that mucosa-treated tracheas can be used for allotransplantation without the use of immunosuppressants.[13] The decellularization of the epithelium and submucosa removes graft immunogenicity while preserving the ECM for regeneration of a functional epithelium. Meanwhile, maintenance of viable chondrocytes may sustain the tracheal cartilage for long-term patency. Our previous work with orthotopically implanted partially decellularized tracheal grafts (PDTGs) using the mouse model demonstrated complete epithelial regeneration by 1 month and maintenance of tracheal patency without stenosis.[14] Therefore, partial decellularization has the potential to meet the requirements of an ideal tracheal replacement.

Although PDTG have shown great promise, major developments are necessary to make this technology a clinically viable option for repairing long-segment tracheal defects. Conventional methods of producing PDTG typically involve time-consuming agitated immersion processing. In addition, current PDTG processing methods have predominantly been in small animal models that do not reflect the scale and properties of the human trachea. Therefore, a user-friendly approach to efficiently generate PDTG using a large animal model is necessary for preclinical research. This necessitates simplifying the process to create PDTG for ease-of-use and improved control over partial decellularization in a system that accommodates a wide range of tracheal dimensions. Furthermore, this practical approach using large animal models needs to be better than conventional agitated immersion methods in producing PDTG to establish a strong foundation prior to animal transplant and clinical studies.

We aim to address this need with a novel 3D printed bioreactor. We have engineered this bioreactor to be scaled for large animal models and use automated dynamic flow for partial decellularization. Here, we explore the feasibility of this 3D printed bioreactor as a simple and tunable system for practically generating PDTG by comparing it to conventional agitated immersion. Our animal model is the New Zealand white rabbit (*Oryctolagus cuniculus*), which is the classic model for pediatric airway reconstruction and thus has a proven track record of serving as a large animal model for tracheal tissue engineering.[9,15,16] We compare native trachea, conventionally-processed PDTG, and bioreactor-processed PDTG by assessing the effect of processing on decellularization, chondrocyte viability, cartilage collagen content, and mechanical properties. These aspects will serve as the validation of whether the 3D printed bioreactor platform can successfully and efficiently produce PDTG for future optimization. The current work sets the stage for subsequent in vivo rabbit studies that will explore the long-term immunogenicity, regeneration, and structural integrity of PDTG produced using the bioreactor.

2 | MATERIALS AND METHODS

2.1 | Animal care and ethics statement

The Institutional Animal Care and Use Committee of the Abigail Wexner Research Institute (Columbus, OH) reviewed, approved, and monitored the protocol (AR21-00021) encompassing this study. The treatment of animals in this study was in accordance with the

standards published by the National Institutes of Health (NIH, Bethesda, MD) and regulations defined in the Animal Welfare Act by the United States Department of Agriculture (Washington, D.C.).

2.2 | Acquisition of tracheal segments

Nine New Zealand white rabbits (*Oryctolagus cuniculus*, Linnaeus, 1758) between 3.4 and 3.6 kg were euthanized with Euthasol. The airways were resected from the larynx to the carina, then 3.5 cm tracheal segments were created. Three tracheas were assigned to each of the native, bioreactor-processed, and conventionally-processed groups. The tracheal segments were immersed in phosphate-buffered saline with 1% penicillin–streptomycin (P/S, Gibco, Thermo Fisher Scientific, Waltham, MA) for transport before processing.

2.3 | Bioreactor fabrication and setup

The bioreactor components were printed using a stereolithography printer (Form 3B+ with clear resin, Formlabs, Somerville, MA) at 50 µm resolution with standard isopropanol rinse and post-processing with 395 nm light. The bioreactor is composed of a tube with two end fittings. All components of the bioreactor and tubing were disinfected with 70% ethanol in distilled water before use. The fitments were first coupled to the trachea with cable ties (Figure 1). The dimensions of these fitments were retained as an adjustable variable to enable customization based on tracheal diameter. This assembly was then inserted into the bioreactor tube and locked into place with a retaining ring. The fitment which does not lock with the retaining ring is free to be adjusted in or out of the tube to fit various tracheal lengths. The assembled bioreactor had intraluminal and extraluminal fluid paths which were then connected to peristaltic pumps (Masterflex L/S, VWR, Radnor, PA), tube clamps, and solution bottles using silicone tubing. The intraluminal chamber drew alternatively from two bottles, one containing Dulbecco's Modified Eagle medium (DMEM) and the second containing a 1% solution of the decellularizing detergent sodium dodecyl sulfate (SDS, Sigma-Aldrich, St. Louis, MO), through a flow splitter and two tube clamps. The solution bottles were vented with gas-permeable syringe filters (0.2 µm, Corning, Corning, NY). The flow into the extraluminal chamber was drawn from a bottle containing DMEM with 10% fetal bovine serum (FBS) and 1% P/S. The solutions pumped through both chambers were maintained at a flow rate of 5 mL/min to minimize shear stress. The bioreactor and solutions were maintained at 37°C and 5% CO_2 with saturating humidity within a cell culture incubator (Fisherbrand Isotemp, Thermo Fisher Scientific).

2.4 | Partial decellularization protocols

The conventional partial decellularization protocol uses surfactant and enzymatic activity combined with agitation and osmotic forces for decellularization. This protocol was adapted from previously published studies.[15–17] Three tracheal segments were subjected to immersion

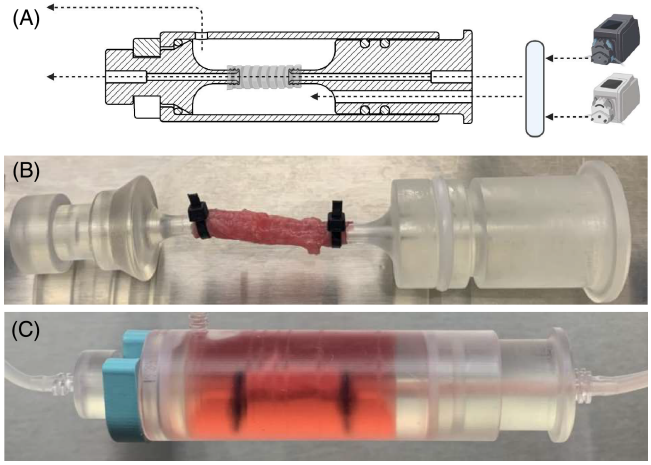

FIGURE 1 Bioreactor design and setup: (A) Cross-section of the bioreactor with mock tracheal segment. The dotted arrows represent the intraluminal and extraluminal flow paths. The pumps are represented on the right with the rectangle representing flexible fluid valving and splitting. (B) Rabbit trachea which has been affixed to the two modular end fittings of the bioreactor. (C) Fully installed bioreactor with connected tubing and media flow.

with 1000 rpm agitation in 1% SDS for 3.75 h, 2% Triton X-100 for 2.5 h, 2000 kU/L DNase in 1 M NaCl for 1.25 h at 37°C, and ddH_2O with 1% penicillin–streptomycin for 2.5 h. These durations were the shortest duration that resulted in complete decellularization of the tracheal epithelium and submucosa. The solutions were maintained at room temperature.

In parallel, three tracheal segments were partially decellularized using the bioreactor. The intraluminal surface of the trachea was exposed to the decellularizing SDS to achieve decellularization of the epithelium and submucosa while the extraluminal surface of the trachea was exposed to culture medium to enable diffusion of nutrients through the sparse adventitia to the cartilage. The intraluminal compartment was exposed to 12 cycles, each cycle consisting of 15 min of 1% SDS followed by 5 min of DMEM, for a total of 4 h. The number of cycles was selected because it was the shortest duration necessary for complete de-epithelialization. The extraluminal compartment was exposed to typical culture conditions with a continuous flow of DMEM with 10% FBS and 1% P/S.

2.5 | Histology and imaging

The tracheal segments were fixed in 10% formalin, embedded in paraffin, and sectioned at 5 µm for transverse imaging of the trachea. Tissue morphology was assessed with hematoxylin and eosin (H&E) staining (Sigma–Aldrich). The effect of partial decellularization on cartilage ECM composition was assessed using Masson's trichrome staining. Collagen staining with Masson's trichrome was selected because collagen is the primary structural macromolecule in cartilage.[18] The images of Masson's trichrome stains were exported as TIFF format to be quantified using the *Automated Fibrosis Analysis Tool* (AFAT) previously published by Gratz et al.[19] The AFAT first filters the images,

applies linear regression to identify white pixels from undetermined pixels, and then uses the k-nearest neighbors algorithm to sort whether each pixel represents the blue pixels of Masson's trichrome collagen staining. First, ImageJ (NIH) was used to select a region-of-interest that encompassed the largest continuous section of cartilage and excluded the perichondrium. Next, these images were uploaded into the AFAT to yield the stain percentage ($\text{Stain percentage} = \frac{\text{Stained tissue pixels}}{\text{Stained tissue pixels} + \text{non-stained tissue pixels}} \times 100$). The pixels categorized as "other" were included in the count of stained tissue since these pixels represented the majority of the hyaline cartilage. Default parameters (5 nearest neighbors and HSV color rules) were used for this analysis.

Chondrocyte viability was evaluated using a live/dead cytotoxicity kit (Invitrogen, Thermo Fisher Scientific). The tracheal segments were immersed in Calcium Green-1, AM (6 μL/mL) and ethidium homodimer-1 (10 μL/mL) at room temperature. The tracheal cartilage was exposed with transverse cuts and then imaged with a confocal microscope at 10× magnification (LSM 700, Zeiss, Oberkochen, Germany). Cells with green fluorescence were considered live and cells with red fluorescence were considered dead or damaged cells. Cellular viability was defined as the percentage of living cells out of total cells ($\text{Viability} = \frac{\text{Live cells}}{\text{Live} + \text{Dead cells}} \times 100$) in a representative field of view. ImageJ was used for cell counting.

2.6 | DNA quantification

The extent of tracheal tissue decellularization was quantified using DNA concentration (ng DNA/mg dry tissue). The whole wet tissue was lyophilized overnight and then weighed. The DNA was first extracted with an extraction kit (DNeasy Blood & Tissue Kit, QIAGEN, Germantown, MD) and then measured with a spectrophotometer (Nanodrop™ 2000c, Thermo Fisher Scientific).

2.7 | Compression testing

The radial compressive strength of the tracheal tissue was quantified using uniaxial compression testing with methods adapted from Jones et al.[20] This testing examines the ability of the trachea to withstand external forces to maintain a patent lumen. A 20 N load cell was attached to a computer-controlled tensile and compression test system (MultiTest 5-I, Mecmesin, West Sussex, United Kingdom). 1 cm tracheal segments were placed sideways on a larger polyethylene block under the load cell assembly such that compression would ultimately cause luminal collapse. 3 mm/min compression was applied until the lumen was 90% ∼ 100% obstructed and the force at 50% luminal obstruction was recorded.

2.8 | Statistical analysis

GraphPad Prism 9 (GraphPad Software Inc., La Jolla, CA) was used for statistical analysis. Tukey's multiple comparison's test was used to test for differences between the native, conventionally-processed, and bioreactor-processed groups. Hypothesis testing results were considered significant if $P < .05$. The figures represent data using scatter plots with means and standard deviations.

3 | RESULTS

3.1 | Conventional and bioreactor processing decellularized the epithelium and submucosa

The effect of the partial decellularization methods was qualitatively assessed using H&E staining (Figure 2). When compared to native trachea, both the conventional immersion and bioreactor processing methods successfully decellularized the epithelium and submucosa, as evident by reduced nuclei and cell bodies, and left the cartilage intact. Next, the tissue DNA content was assessed. This measure has previously been used to quantify the extent of decellularization.[21] Native trachea had a DNA content of 1.02 μg/mg (SD 0.26 μg/mg), conventionally-processed trachea had an average of 1.31 μg/mg (SD 0.27 μg/mg), and bioreactor-processed trachea had an average of 0.84 μg/mg (SD 0.23 μg/mg). There were no differences between these groups (native vs. conventional: $P = .39$; native vs. bioreactor: $P = .68$; conventional vs. bioreactor: $P = .13$).

3.2 | Bioreactor processing maintained chondrocyte viability

Live/dead assay measured chondrocyte viability after partial decellularization (Figure 3). Native trachea had an average chondrocyte viability of 96.2% (SD 1.9%) which was greater than the viability of 0% (SD 0%) seen in conventionally processed trachea ($P = .0002$). In contrast, bioreactor processing resulted in 79.39% (SD 20.8%) viability which is comparable to native trachea ($P = .28$). Bioreactor processing also resulted in better chondrocyte viability compared to conventionally-processed trachea ($P = .0005$).

3.3 | Conventional and bioreactor processing preserved cartilage collagen content

The collagen content of the tracheal cartilage was assessed using Masson's trichrome staining and the AFAT algorithm (Figure 4). The AFAT algorithm yielded the approximate percentage of cartilage stained blue by Masson's trichrome staining. Native trachea demonstrated an average of 89.65% (SD 1.39%) staining while conventionally-processed trachea had 84.18% (SD 8.24%) staining and bioreactor-processed trachea had 74.50% (SD 7.27%) staining. The results seen after conventional processing and bioreactor processing did not differ from native trachea ($P = .58$ and $P = .062$, respectively) and between each other ($P = .23$).

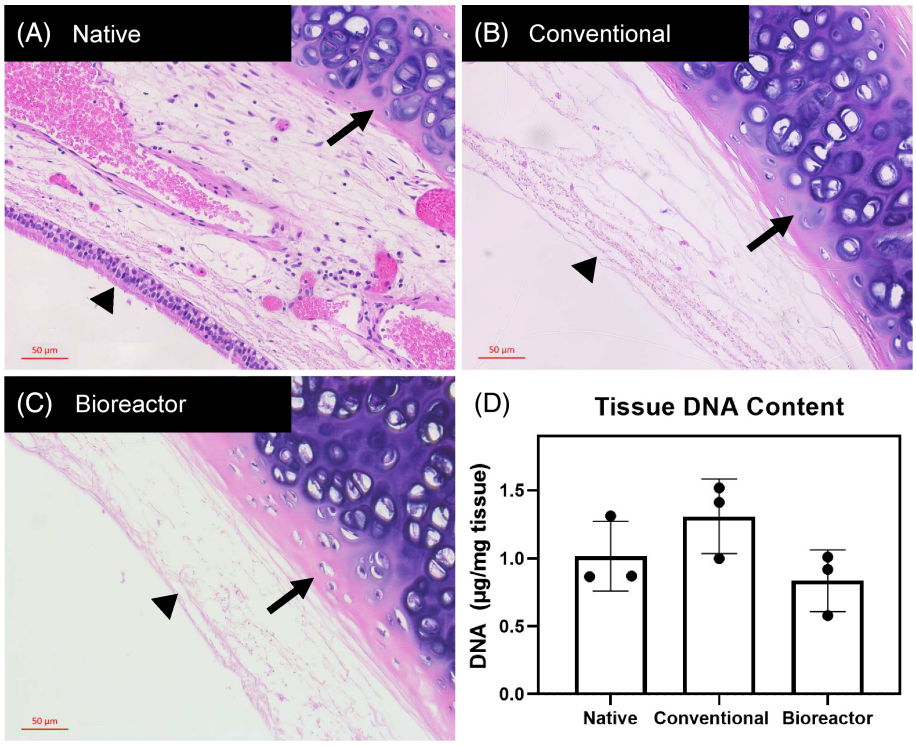

FIGURE 2 H&E staining and DNA content assay: (A–C) Representative axial H&E images of native and processed trachea. The triangles denote the epithelium while the arrows denote the cartilage. (D) DNA content assay results which demonstrate no differences between the groups.

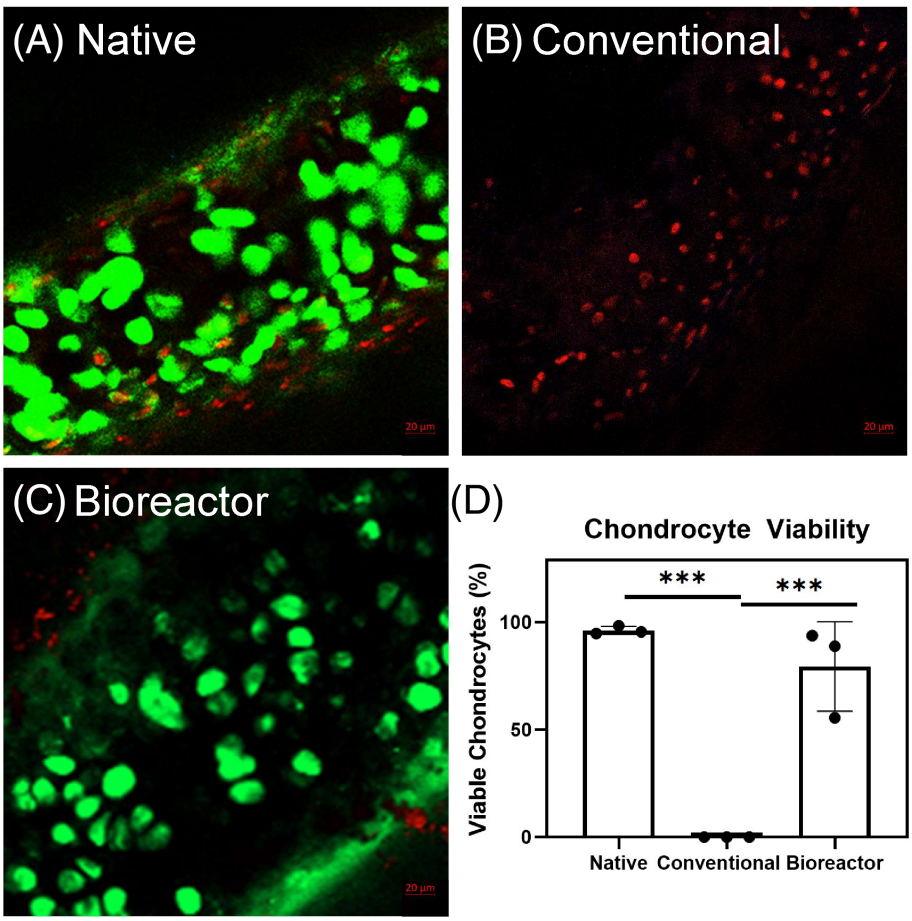

FIGURE 3 Live/dead assay and viability quantification: (A–C) Representative axial live/dead images of native and processed trachea. (D) Quantified viability demonstrating that conventional processing results in partially decellularized tracheal grafts with chondrocyte viability lower than that of native and bioreactor-processed trachea. (*** denotes significance with $P \leq .001$).

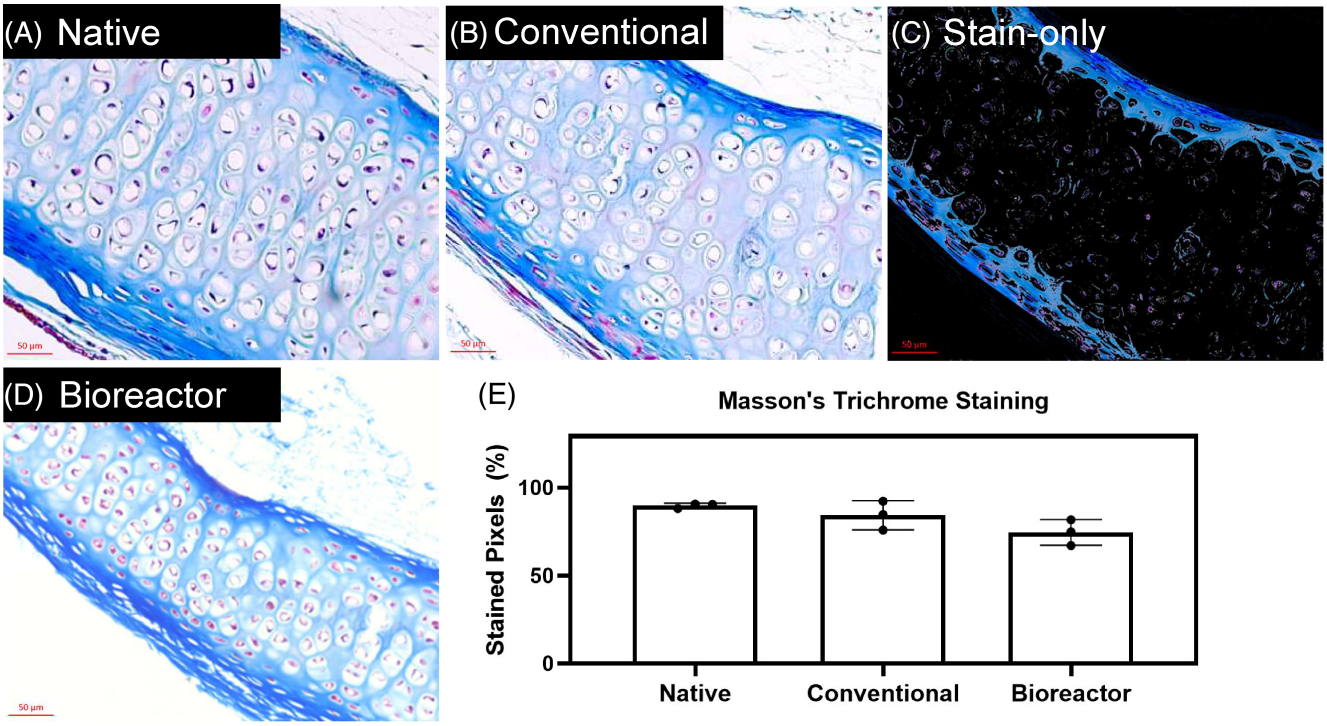

FIGURE 4 Masson's trichrome: (A, B, D) Representative axial images of native and processed trachea stained with Masson's trichrome. (C) A representative cropped and stain-only image of (B) processed using the AFAT algorithm. (E) Stain percentages which demonstrate no differences between the groups.

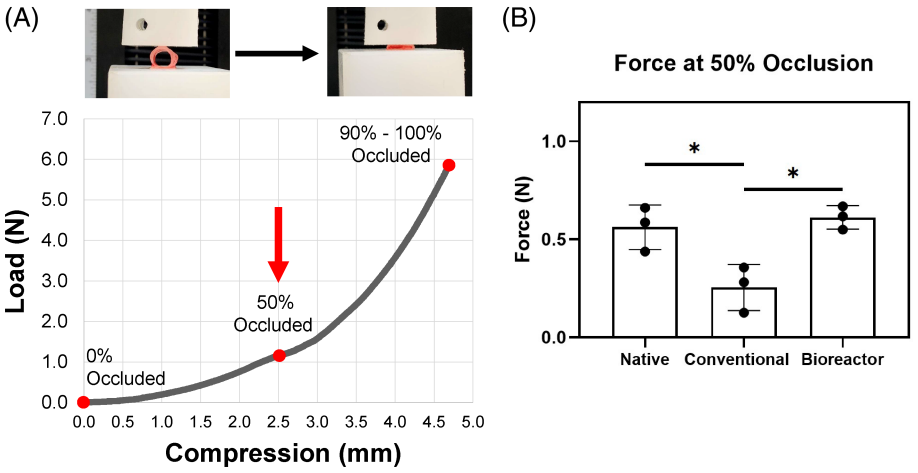

FIGURE 5 Compression testing method and results: (A) Example load-compression graph with images demonstrating correlated tracheal occlusion. The arrow shows the datum at 50% occlusion which was used to compare between groups. (B) Force at 50% occlusion which demonstrates that conventional processing results in partially decellularized tracheal grafts that occlude at lower loads when compared to native and bioreactor-processed trachea. (* denotes significance with $P \leq .05$).

3.4 | Conventional and bioreactor processing preserved tracheal mechanical strength

The force necessary for 50% luminal obstruction was used to compare the mechanical strength of the trachea (Figure 5). The average force resisted by native trachea was 0.56 N (SD 0.11 N), conventionally-processed trachea was 0.26 N (SD 0.12 N), and bioreactor-processed trachea was 0.61 N (SD 0.06 N). The average force measured with the conventionally-processed trachea was lower than that of both native and bioreactor-processed trachea ($P = .02$ and $P = .01$, respectively). Meanwhile, the average force did not differ between the native and bioreactor-processed trachea ($P = .82$).

4 | DISCUSSION

Bioreactors offer significant practical advantages because they enable precise control of culturing conditions and automation.[22] Bioreactors have been successfully used to de-epithelialized porcine tracheal allografts and computational fluid dynamics have been used to optimize graft recellularization specifically for long-segment tracheal grafts.[23,24] The compelling need for an effective method for repairing long-segment tracheal defects motivated us to engineer a novel 3D printed bioreactor that is user-friendly for clinical use while being an ideal platform for producing PDTG for preclinical studies.

Our 3D printed bioreactor offers a simple four-piece modular design (Figure 1). The 3D printed components can be rapidly produced at low cost and easily hand-assembled for an accessible and scalable platform that fits a wide range of tracheal dimensions. Preexisting bioreactors lack these features because they involve complex assembly and lack full adjustability. These features lend to the practicality and flexibility required for clinical research of not only PDTG, but potentially other types of organ grafts. The tube-like design makes it possible to externally rotate the bioreactor which enables uniform delivery of cells for reseeding or other particles for toxicology and pharmaceutical studies. The modular end fittings bring with them almost endless possibilities for culturing any organ or graft geometry. The application we chose here is to produce rabbit PDTG because the bioreactor platform lends to complex processing at human scales.

We validated this platform by generating rabbit PDTG that had chondrocyte viability and collagen content similar to that of native tracheal cartilage while requiring shorter processing times than conventional non-bioreactor processing (Figures 3 and 4). This increased efficiency likely stemmed from the benefits of dynamic flow, which enhanced tissue SDS exposure, SDS replenishment, and removal of cellular debris.[25] Furthermore, using the bioreactor resulted in PDTG that maintained mechanical properties similar to that of native trachea (Figure 5). The maintenance of these critical characteristics may help contribute to post-transplant cartilage maintenance and airway patency.[11,18,26] However, the bioreactor processing did not result in significantly reduced DNA content. This finding demonstrates that tissue DNA content is not a suitable measure for partially decellularized grafts since a population of cells are intentionally preserved.[21] These results show that the bioreactor processing is suitable for efficiently creating PDTG that can be predicted to have favorable long-term airway patency in future transplant studies.

There is yet much to explore in terms of the flexibility and capability of bioreactor processing in the context of transplantation. The bioreactor enables adjustable flow rates and flexible processing regimens which can further optimize PDTG generation. The impact of these variables needs to be explored, especially with a focus on how bioreactor processing affects tissue regeneration. Our previous PDTG studies with the mouse model showed successful graft epithelialization, vascularization, increased chondrocyte viability, and maintenance of patency 28 days after orthotopic segmental tracheal replacement.[14] Splinted PDTG have been shown to successfully revascularize with no difference in the number or size of vessels compared to controls.[27] In addition, long-term studies using rabbit PDTG created with immersion and sonication have demonstrated successful integration and animal survival up to 2 years.[28] These results show that there already is promise in the long-term viability and functionality of PDTG. Therefore, optimizing bioreactor-generated PDTG with long-term rabbit transplant studies is the focus of our upcoming experiments and the next step to push this novel technology closer to clinical adaptation. We anticipate that these studies will determine the long-term functional superiority of the bioreactor-processed PDTG by assessing the in vivo maintenance of low immunogenicity, inducement of tissue regeneration, and sustained mechanical integrity.

Looking toward the future, the ideal tracheal graft will be available for all pediatric to adult patients. One anticipated challenge is the difference in scale between the adult human and rabbit model demonstrated here. For example, a graft from an adult human donor will have thicker tissues which will affect the permeation of the reagents and will necessitate different protocols and potentially different chemicals. In addition, values such as the permeability coefficients may significantly differ based on the age of the human donor due to differences in tissue composition.[29] This challenge can be addressed by further optimizing the processing parameters based on the graft's characteristics, whether by computational modeling or empirically. Thankfully, the bioreactor platform lends to the consistency and automatability required for such developments and we believe that it has great potential for use in future studies that explore the next generation of tissue engineering.

5 | CONCLUSION

Partially decellularized tracheal grafts have the potential to be used to repair long-segment tracheal defects. This technology has been validated using mouse models, but clinical translation necessitates further study using large animal models and processing more amenable to clinical use. A novel 3D printed bioreactor platform was demonstrated with rabbit tracheas to be more efficient at removing cells in epithelium and submucosa while maintaining chondrocyte viability and cartilage compared to conventional protocols. This 3D printed bioreactor offers flexibility and adjustability favorable to creating PDTG for preclinical transplant studies.

ACKNOWLEDGMENTS

We would like to thank Dr. Jed Johnson and Joey Huddle at Nanofiber Solutions, LLC (Dublin, OH, USA) for helping with the mechanical testing of the trachea.

FUNDING INFORMATION

This work was supported in part by an Alpha Omega Alpha Carolyn L. Kuckein Student Research Fellowship (W.Y.B.) and the National Institutes of Health NHLBI R01HL157039 (T.C.).

CONFLICT OF INTEREST STATEMENT

A provisional patent application titled "Modular Adjustable Bioreactor for Decellularization and Cell Seeding" is described in US Provisional Application No. 63/384028 filed in the United States Patent and Trademark Office on November 16, 2022. Tendy Chiang, Woo Yul Byun, and Lumei Liu share equal inventorship.

ORCID

Woo Yul Byun https://orcid.org/0000-0001-8686-638X
Lumei Liu https://orcid.org/0000-0001-9849-6881
Zheng Hong Tan https://orcid.org/0000-0003-1571-464X

Kyle VanKoevering https://orcid.org/0000-0001-5921-7042
Tendy Chiang https://orcid.org/0000-0003-1448-5873

REFERENCES

1. Grillo HC. Tracheal replacement: a critical review. *Ann Thorac Surg*. 2002;73(6):1995-2004. doi:10.1016/s0003-4975(02)03564-6
2. Hinderer S, Schenke-Layland K. Tracheal tissue engineering: building on a strong foundation. *Expert Rev Med Devices*. 2013;10(1):33-35. doi:10.1586/erd.12.74
3. Fabre D, Kolb F, Fadel E, et al. Successful tracheal replacement in humans using autologous tissues: an 8-year experience. *Ann Thorac Surg*. 2013;96(4):1146-1155. doi:10.1016/j.athoracsur.2013.05.073
4. Kashiwa K, Kobayashi S, Tono H, Nohara T, Honda T, Sakurai S. Reconstruction of the cervical trachea using a prefabricated cortico-periosteal flap from the femur. *Ann Plast Surg*. 2009;62(6):633-636. doi:10.1097/SAP.0b013e31817f023e
5. Al-Khudari S, Sharma S, Young W, Stapp R, Ghanem TA. Osteocutaneous radial forearm reconstruction of large partial cricotracheal defects. *Head Neck*. 2013;35(8):E254-E257. doi:10.1002/hed.23088
6. Wurtz A, Porte H, Conti M, et al. Tracheal replacement with aortic allografts. *N Engl J Med*. 2006;355(18):1938-1940. doi:10.1056/NEJMc066336
7. Delaere P, Vranckx J, Verleden G, de Leyn P, van Raemdonck D, Leuven Tracheal Transplant Group. Tracheal allotransplantation after withdrawal of immunosuppressive therapy. *N Engl J Med*. 2010;362(2):138-145. doi:10.1056/NEJMoa0810653
8. Klepetko W, Marta GM, Wisser W, et al. Heterotopic tracheal transplantation with omentum wrapping in the abdominal position preserves functional and structural integrity of a human tracheal allograft. *J Thorac Cardiovasc Surg*. 2004;127(3):862-867. doi:10.1016/j.jtcvs.2003.07.050
9. Abdülcemal Işik U, Seren E, Kaklikkaya I, et al. Prosthetic reconstruction of the trachea in rabbit. *J Cardiovasc Surg (Torino)*. 2002;43(2):281-286.
10. Dharmadhikari S, Liu L, Shontz K, et al. Deconstructing tissue engineered trachea: assessing the role of synthetic scaffolds, segmental replacement and cell seeding on graft performance. *Acta Biomater*. 2020;102:181-191. doi:10.1016/j.actbio.2019.11.008
11. Liu Y, Nakamura T, Sekine T, et al. New type of tracheal bioartificial organ treated with detergent: maintaining cartilage viability is necessary for successful immunosuppressant free allotransplantation. *ASAIO J*. 2002;48(1):21-25. doi:10.1097/00002480-200201000-00006
12. Liu Y, Nakamura T, Yamamoto Y, et al. Immunosuppressant-free allotransplantation of the trachea: the antigenicity of tracheal grafts can be reduced by removing the epithelium and mixed glands from the graft by detergent treatment. *J Thorac Cardiovasc Surg*. 2000;120(1):108-114. doi:10.1067/mtc.2000.106655
13. Wang J, Zhang H, Sun Y, Liu P, Li S, Cui P. Mechanical properties of de-epithelialized tracheal allografts. *J Thorac Dis*. 2021;13(2):1066-1074. doi:10.21037/jtd-20-2739
14. Liu L, Dharmadhikari S, Shontz KM, et al. Regeneration of partially decellularized tracheal scaffolds in a mouse model of orthotopic tracheal replacement. *J Tissue Eng*. 2021;12:17417. doi:10.1177/20417314211017417
15. Lange P, Shah H, Birchall M, Sibbons P, Ansari T. Characterization of a biologically derived rabbit tracheal scaffold. *J Biomed Mater Res B Appl Biomater*. 2017;105(7):2126-2135. doi:10.1002/jbm.b.33741
16. Maughan EF, Butler CR, Crowley C, et al. A comparison of tracheal scaffold strategies for pediatric transplantation in a rabbit model. *Laryngoscope*. 2017;127(12):E449-E457. doi:10.1002/lary.26611
17. Zhong Y, Jiang A, Sun F, et al. A comparative study of the effects of different decellularization methods and Genipin-cross-linking on the properties of tracheal matrices. *Tissue Eng Regen Med*. 2018;16(1):39-50. doi:10.1007/s13770-018-0170-6
18. Liu L, Stephens B, Bergman M, May A, Chiang T. Role of collagen in airway mechanics. *Bioengineering (Basel)*. 2021;8(1):13. doi:10.3390/bioengineering8010013
19. Gratz D, Winkle AJ, Dalic A, Unudurthi SD, Hund TJ. Computational tools for automated histological image analysis and quantification in cardiac tissue. *MethodsX*. 2019;7:22-34. doi:10.1016/j.mex.2019.11.028
20. Jones MC, Rueggeberg FA, Faircloth HA, et al. Defining the biomechanical properties of the rabbit trachea. *Laryngoscope*. 2014;124(10):2352-2358. doi:10.1002/lary.24739
21. Crapo PM, Gilbert TW, Badylak SF. An overview of tissue and whole organ decellularization processes. *Biomaterials*. 2011;32(12):3233-3243. doi:10.1016/j.biomaterials.2011.01.057
22. Lim D, Renteria ES, Sime DS, et al. Bioreactor design and validation for manufacturing strategies in tissue engineering. *Biodes Manuf*. 2022;5(1):43-63. doi:10.1007/s42242-021-00154-3
23. Aoki FG, Varma R, Marin-Araujo AE, et al. De-epithelialization of porcine tracheal allografts as an approach for tracheal tissue engineering. *Sci Rep*. 2019;9(1):12034. doi:10.1038/s41598-019-48450-4
24. Lee H, Marin-Araujo AE, Aoki FG, et al. Computational fluid dynamics for enhanced tracheal bioreactor design and long-segment graft recellularization. *Sci Rep*. 2021;11(1):1187. doi:10.1038/s41598-020-80841-w
25. Montoya CV, McFetridge PS. Preparation of ex vivo-based biomaterials using convective flow decellularization. *Tissue Eng Part C Methods*. 2009;15(2):191-200. doi:10.1089/ten.tec.2008.0372
26. Park JH, Hong JM, Ju YM, et al. A novel tissue-engineered trachea with a mechanical behavior similar to native trachea. *Biomaterials*. 2015;62:106-115. doi:10.1016/j.biomaterials.2015.05.008
27. Nyirjesy SC, Yu J, Dharmadhikari S, et al. Successful early neovascularization in composite tracheal grafts. *Otolaryngol Head Neck Surg*. 2023;169:1040. doi:10.1002/ohn.350
28. Dang LH, Tseng Y, Tseng H, Hung SH. Partial decellularization for segmental tracheal scaffold tissue engineering: a preliminary study in rabbits. *Biomolecules*. 2021;11(6):866. doi:10.3390/biom11060866
29. Roberts CR, Paré PD. Composition changes in human tracheal cartilage in growth and aging, including changes in proteoglycan structure. *Am J Physiol*. 1991;261(2):L92-L101. doi:10.1152/ajplung.1991.261.2.L92

How to cite this article: Byun WY, Liu L, Palutsis A, et al. Dynamic flow for efficient partial decellularization of tracheal grafts: A preliminary rabbit study. *Laryngoscope Investigative Otolaryngology*. 2024;9(2):e1247. doi:10.1002/lio2.1247